Preparation of carbon microparticle assemblies from phenolic resin using an inverse opal templating method

Guoqing Guan · Katsuki Kusakabe · Haruka Ozono · Masatsugu Taneda · Masato Uehara · Hideaki Maeda

Abstract Three-dimensionally (3D) well-ordered carbon microparticle assemblies with different particle morphologies were fabricated by infiltration of phenolic resin solution into SiO_2 inverse opal structures and subsequent carbonization. The effect of the phenolic resin solution concentration and the carbonization temperature on the morphology of the fabricated carbon microparticles was investigated. At a carbonization temperature of 1000 °C, carbon microparticles with interlocked bridges were obtained when the concentration of phenolic resin solution is 40 wt% and hollow carbon microparticles with opened window channels were obtained at a concentration of 30–35 wt%. When the carbonization temperature was decreased to 500 °C, carbon microparticles with interlocked bridges also were observed, even when the phenolic resin concentration was 30 wt%. The structures and properties of the carbon microparticles and their assemblies were characterized using SEM, XRD, and N_2 adsorption.

Introduction

The synthesis of carbon particles with controlled size and shape distributions has attracted significant attention

G. Guan · K. Kusakabe (✉) · H. Ozono · M. Taneda
Department of Living Environmental Science, Fukuoka
Women's University, 1-1-1 Kasumigaoka, Higashi-ku, Fukuoka
813-8529, Japan
e-mail: kusakabe@fwu.ac.jp

H. Ozono · M. Uehara · H. Maeda
Nanotechnology Research Institute, National Institute of
Advanced Industrial Science and Technology (AIST), 807-1
Shuku-machi, Tosu, Saga 841-0052, Japan

because of the potential use of carbon particles in a variety of applications, including catalyst support, gas storage, drug delivery, and high-capacity negative electrode materials [1–7]. Fine carbon particles can be classified into three categories based on size: nanosized (<100 nm), sub-microsized (0.1–1 μm) and microsized (1–10 μm) particles. Nanosized carbon particles usually are synthesized using a general chemical and/or physical method. Sub-microsized and microsized carbon particles are necessary for a number of practical applications. Moreover, the morphology of such particles also is important. To date, general chemical methods for synthesizing mono-dispersed, well-shaped carbon particles with dimensions ranging from 0.1–1 μm remains a challenge for materials scientists. Fuertes [8] fabricated mesoporous carbon particles of all three sizes, with large surface areas and pore volumes, by selecting different silica templates. Although the micrometric carbon particles showed a perfectly spherical morphology and a unimodal pore size distribution, the particle size distribution was nonuniform and the polydispersity was not explicitly reported. Tosheva et al. [9] used an ion-exchange resin template to control both shape and pore structure in the synthesis of microsized carbon particles. Using this method, particle size also was nonuniform. Su et al. [10] fabricated mono-dispersed, hollow carbon spheres by chemical vapor deposition (CVD) of benzene or acetonitrile, using silica spheres as templates. However, the carbon precursor of CVD is limited.

Recently, the ordered three-dimensional structure resulting from self-arrangement of monodispersed, sub-microsized spheres has attracted significant attention [11–13]. Such materials are called colloidal crystal, or opal, and are useful in a variety of applications, such as photonic crystals, size-exclusion chromatography, catalysis, adsorption, and other emerging nanotechnologies, due

to their uniform physical and chemical properties. However, to date, only polymer microspheres, such as polystyrene (PS) and polymethylmethacrylate (PMMA) microspheres, and silica microspheres can be prepared using self-arrangement. The infilling of the opal structure with a precursor also has been established as a promising method for fabrication of inverse opal structures with ordered macropores. The inverse opal structure can, in turn, be used as a template to make an array of uniform microsized particles, which are generally difficult to fabricate using a chemical and/or physical method. Using this double template method, Colvin et al. [14] prepared macroporous polymer inverse opals (i.e., PS and PMMA) by using silica opal as a template, and the uniform and interconnected void of the inverse opal were used to generate a wide variety of highly monodispersed inorganic (i.e., TiO_2, ZrO_2, Al_2O_3, CdS, AgCl), polymeric (i.e., polypyrrole, poly(p-phenylenevinylene) (PPV)) and metallic (i.e., Au and Ni) solid, core-shell and hollow microparticle arrays. Ozin et al. [15] used the same method to obtain monodispersed silica microspheres by infiltration of silicatropic liquid crystals into polymer inverse opal. Using carbon inverse opal as a template, Lei et al. [16] fabricated TiO_2, Nd_2O_3, SiO_2 and Al_2O_3 hollow spheres. Yang et al. [17] developed a polymer inverse opal with macropores interconnected by windows that were large enough for small PS latex particles, approximately 500 nm in diameter, to pass through. After the large pores were filled with the PS particles and dried, the silica or titania alkoxide precursor was infiltrated into the interstices formed between the latex particles. Finally, the polymer matrix and latex particles were removed by calcination in air, yielding ordered macroporous SiO_2 or TiO_2 microparticles. Kim et al. [18] fabricated ordered assemblies of hollow SiC- and filled SiCN-microspheres using carbon inverse opal as a template and polymethylsilane and polysilazane as SiC and SiCN precursors, respectively. In our previous study [19], a three-dimensionally (3D) well-ordered assembly comprised of silicon oxycarbide (SiO_xC_y) microparticles was fabricated by an infiltration process, using SiO_2 inverse opal structures as templates and polycarbosilane as the precursor. As for carbon microparticles and their assemblies, Zhao et al. [20] reported the preparation of 3D macroporous carbon, carbon capsules, solid carbon spheres and walnut-like carbon nanostructures using silica inverse opals as templates and sucrose as the precursor. The carbon materials produced from sucrose usually are amorphous and exhibit poor electronic conductivity in comparison with those synthesized from aromatic precursors [5, 6, 21]. Phenolic resins are a large family of low-cost polymers composed from a variety of aromatic structures. When phenolic resin was carbonized at 800 °C, graphitic microporous materials with relatively high sorption capacity and

molecular sieve properties were obtained [22, 23]. In the present study, a well-defined SiO_2 inverse opal was prepared by the infiltration of silica sol into the void of the PMMA opal structure. Phenolic resin solution infiltrated the prepared SiO_2 inverse opal under reduced pressure. The effect of the phenolic resin solution concentration and the carbonization conditions on the morphology and three-dimensional ordered assemblies of the synthesized carbon microparticles was investigated.

Experimental

Fabrication of well-defined 3D SiO_2 inverse opal

Methods described previously [19] were used to fabricate well-defined 3D SiO_2 inverse opal. Stable SiO_2 sol was prepared by hydrolysis and condensation of a solution containing tetraethylorthosilicate (TEOS, 96%, $Si(OC_2H_5)_4$; Tokyo Kasei Kogyo Co., LTD), ethyl alcohol (EtOH; Wako), and hydrochloric acid (37%HCl; Wako) with a molar composition of 1.0TEOS:20EtOH:0.02HCl:$5H_2O$. Then, infiltration of the interstitial void of a PMMA opal with a particle size of 260 nm, which had been prepared using a gravitational method, by the prepared SiO_2 sol was performed in a glove box that had been purged with nitrogen. After drying for 24 h, the PMMA-silica xerogel composite was calcinated at 550 °C for 10 h in air with a ramping rate of 1 °C/min. As a result of thermal decomposition of the PMMA particles, the well-defined SiO_2 inverse opal was fabricated.

Infiltration of phenolic resin solution into SiO_2 inverse opal

Phenolic resin (PR-54562, 60 wt% in methanol, Sumitomo Bakelite Co.,Ltd, Japan) was the precursor used to prepare the carbon microparticles. The concentration of the phenolic resin solution was adjusted to 20, 30, 35, and 40 wt% by dilution with methanol (Aldrich). The viscosities of the diluted phenolic resin solutions were determined with a torsion-balanced, oscillation type viscometer (VM-1G, CBC Materials Co., Ltd, Japan). Then, the prepared SiO_2 inverse opal was placed in a two-neck flask connected to a vacuum pump. After evacuation, the prescribed amount of phenolic resin solution was injected into the inverse opal with a syringe through a rubber cap on the flask and was then dried in air at 160 °C for 1 h. Then, the solid samples were heated in dry N_2 to 500, 800, and 1000 °C, at a ramping rate of 1 °C/min and held at a constant temperature for 1 h for carbonization.

Silica dissolution in hydrofluoric acid and characterization

The resulting carbon–SiO$_2$ composite was treated with 20% aqueous HF for 24 h without stirring, followed by filtration and repeated washing with distilled water. The morphologies of the synthesized carbon microparticles and their assemblies were observed with a scanning electron microscope (SEM, Hitachi, S-5200). Powder X-ray diffraction (XRD) patterns of carbon microparticles were recorded on a Rigaku RINT-2500 diffractometer using CuKα radiation ($\lambda = 0.15418$ nm) generated at 40 kV and 30 mA. Nitrogen absorption/desorption isotherm measurements were done at 77 K on a Micrometritics ASAP 2010 gas sorptometer. Prior to the measurements, the samples were degassed at 140 °C for 12 h. The specific surface area was calculated by the Brunauer-Emmett-Teller (BET) method using the adsorption data in a P/P$_0$ range of 0.03 to 0.2.

Results and discussion

### The structure of well-defined carbon microparticle assembly

As reported in the literature [24], PMMA spheres can self-arrange to simultaneously form hexagonal close-packed (hcp) and face-centered cubic (fcc) structures when using the gravitational sedimentation method to prepare the opal structure. Bolhuis [25] suggested that the hcp structure is energetically preferred over the fcc structure, although the energy difference between them is small. In the present study, the hcp structure was primary in the prepared PMMA opal. However, the fcc structure frequently was observed in the opal structure. When the PMMA opal was used as the template, the resulting SiO$_2$ inverse opals exhibited the corresponding hcp and fcc structures, as shown in the insets of Fig. 1a and c, respectively. As a result, when this type of SiO$_2$ inverse opal was used as the template, the same hcp (Fig. 1a, b) and fcc (Fig. 1c, d) structures were observed for the carbon microparticle array that was synthesized using the 40 wt% phenolic resin solution and a carbonization temperature of 1000 °C.

Although the shape of the well-ordered carbon microparticle assembly was almost a replica of the original close-packed PMMA microspheres, the average size of the carbon particles (243 nm) was smaller than that of the PMMA particles (260 nm). As discussed in our previous report [19], the shrinkage was attributed to two processes. First, the shrinkage of the SiO$_2$ inverse opal structure occurred during the calcination at 550 °C. Second, infiltrated phenolic resin in the SiO$_2$ inverse opal shrank again during the carbonization process.

As indicated by the arrows in Fig. 1, carbon bridges between neighboring microparticles or traces of the removed bridges can be clearly seen on the fractured section of the carbon assembly. These carbon bridges were formed in the windows between the spherical air spaces in the inverse opals. The shape of the bridges was similar to that of bridges in the well-ordered SiO$_x$C$_y$ assembly [19]. In this assembly, twelve bridges may symmetrically form on the surface of single microparticle inside the packed block for both hcp and fcc structures. The diameter of the connecting bridges was about 60 nm, coinciding with the connecting pore size in the SiO$_2$ inverse opal. These

Fig. 1 SEM images of synthesized carbon microparticle arrays with hcp (**a**, **b**) and fcc (**c**, **d**) structures. Insets show corresponding SiO$_2$ inverse opals structures. The concentration of infiltrated phenolic resin in methanol was 40 wt% with a viscosity of 2.43 mPa s. Carbonization at 1000 °C under nitrogen gas flow for 1 h. The arrows indicate the contact points with the neighboring carbon microparticles
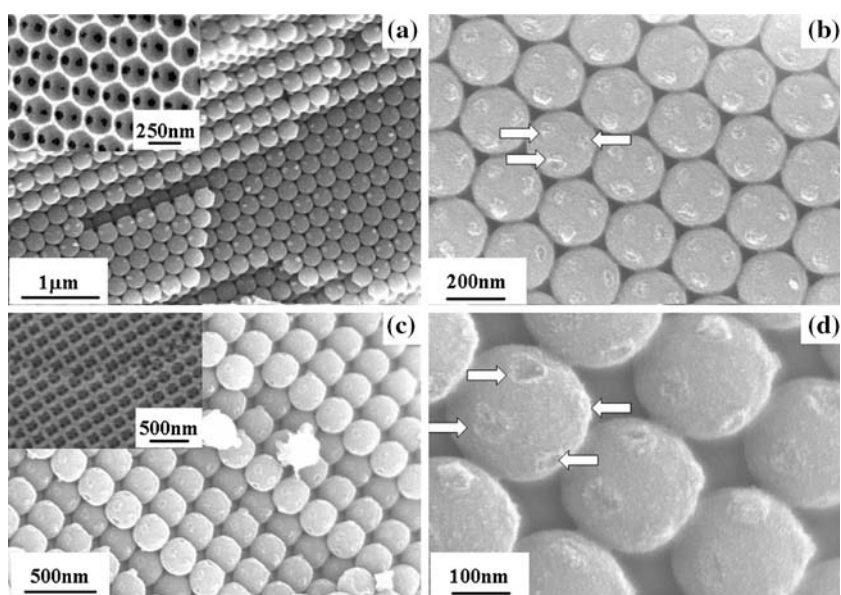
bridges significantly enhanced the mechanical strength of the fabricated carbon microparticle assembly.

In the 3-D well-ordered carbon assembly, the diameter of the maximum circles formed at the intersections of three carbon microparticles in hcp structures and four carbon microparticles in fcc structures were calculated to be 38 and 100 nm, respectively, based on simple geometry. Carbon microparticle assemblies with interpores of different nanosizes could be fabricated when different sizes of original PMMA microparticles were used. Therefore, this procedure could provide a promising alternative to conventional nanofabrication for creating carbon sieving structures which have applications for nanofluidic devices.

### The effect of viscosities of phenolic resin solution

The viscosity of the phenolic resin solution was adjusted to 1.56, 2.01, 2.24, and 2.43 mPa s, corresponding to concentrations of 20, 30, 35, and 40 wt%, respectively. The phenolic resin solution of low viscosity easily infiltrated the voids of SiO_2 inverse opals. Accordingly, the morphology of the obtained particle arrays was changed by altering the concentrations of the infiltrated precursors. The effect of the phenolic resin solution concentration on the morphology of the carbon microparticle assemblies was investigated. Figure 2 shows the SEM images of carbon materials carbonized at 1000 °C. The carbon shell were observed when the phenolic resin solution with a viscosity of 1.56 mPa s was used (Fig. 2a). When the viscosity increased to 2.01 mPa s, carbon spheres with open windows at the contact points with the neighboring particles were obtained (Fig. 2b). When the viscosity increased

further to 2.24 mPa s, some of the open pores closed (Fig. 2c). Finally, when the viscosity was increased to 2.43 mPa s, carbon spheres with intact surface morphology similar to that of the original PMMA microspheres were obtained (Fig. 2d). Figure 3 shows the images of carbon infiltrated SiO_2 inverse opals before silica dissolution in hydrofluoric acid. It is found that the extent of carbon filled the void of SiO_2 inverse opal increased with the increasing of the concentration of the phenolic resin solution. However, it should be noted that when the viscosity of the phenolic resin solution exceeded 3.0 mPa s, infiltration of the SiO_2 inverse opals, even under reduced pressure, was difficult. These phenomena have been observed previously during preparation of other microparticle arrays using this method [14–20]. As a result, the morphology of carbon microparticles could be adjusted by changing the concentration of the phenolic resin solution.

The effect of carbonization temperatures

Figure 4 shows the morphologies of carbon microparticle assemblies fabricated at different temperatures when the phenolic resin solution with a viscosity of 2.01 mPa s was used. At a carbonization temperature of 500 °C, a carbon microparticle assembly with an intact surface morphology was obtained (Fig. 4a). The carbon microparticles obtained at 800 °C had interlocked windows (Fig. 4b, c). When the temperature was increased to 1000 °C, particle size decreased slightly, while the open window size increased a little, suggesting that shrinkage of carbon microparticles had occurred (Fig. 4d).


Fig. 2 SEM images of synthesized carbon microparticle arrays fabricated using different concentrations of phenolic resin in methanol: (**a**) 20 wt%; (**b**) 30 wt%; (**c**) 35 wt%; and (**d**) 40 wt%. Carbonization at 1000 °C under nitrogen gas flow for 1 h
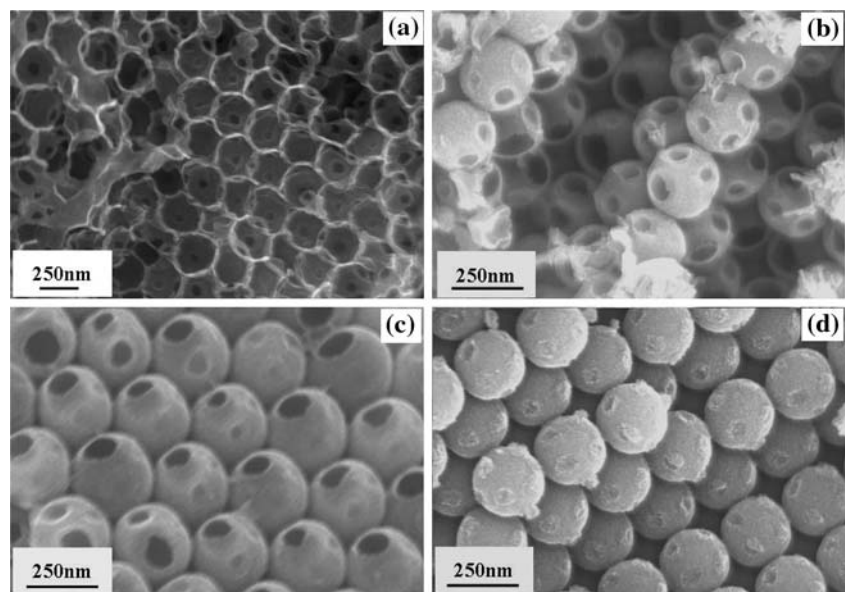
Fig. 3 SEM images of SiO$_2$ inverse opal (**a**) and the carbon infilled SiO$_2$ inverse opals before silica dissolution in hydrofluoric acid when using different concentrations of phenolic resin in methanol: (**b**) 30 wt%; (**c**) 35 wt%; and (**d**) 40 wt%. Carbonization at 1000 °C under nitrogen gas flow for 1 h
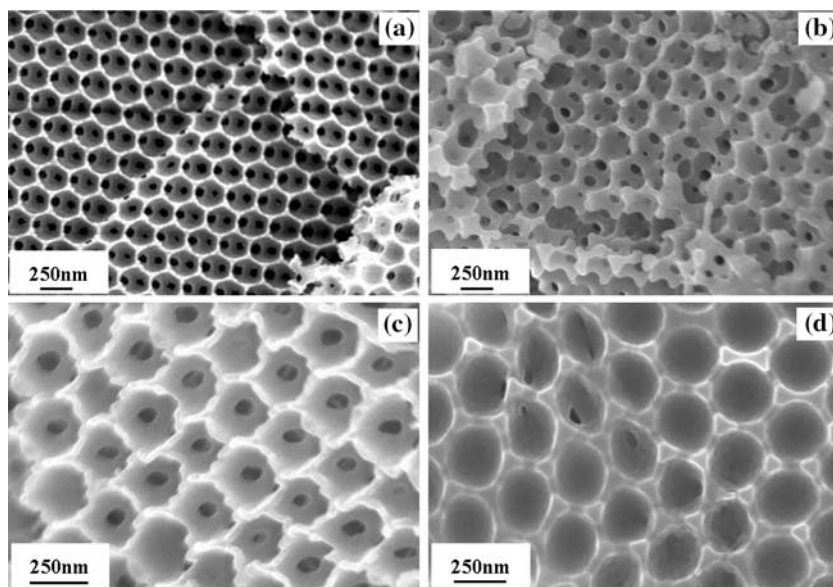

Fig. 4 SEM images of carbon microparticle arrays when carbonized under nitrogen gas flow for 1 h. at different temparaues: (**a**) 500 °C; (**b**) 800 °C (hcp structure); (**c**) 800 °C (fcc structure); (**d**) 1000 °C. The concentration of phenolic resin solution was 30 wt% with a viscosity of 2.01 mPa s
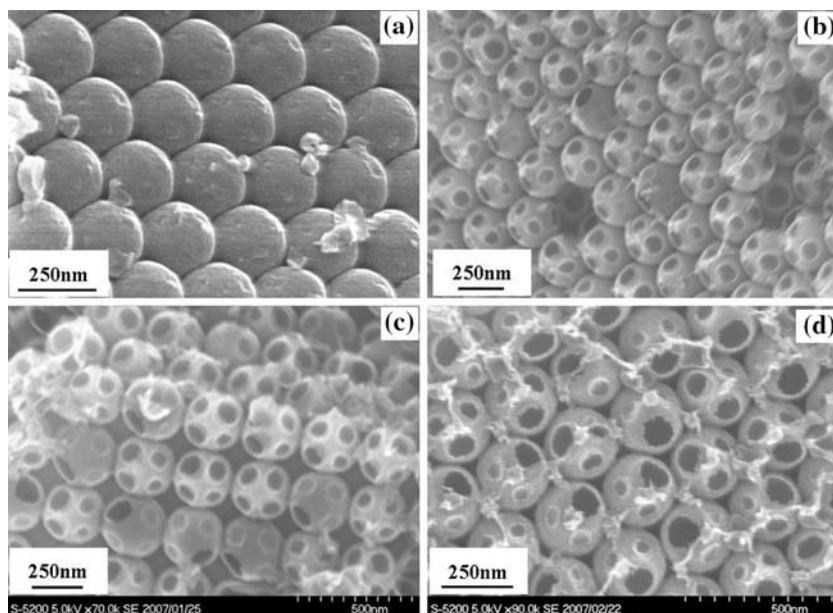

Properties of carbon microparticles

The X-ray diffraction patterns of the samples carbonized at various temperatures are shown in Fig. 5. No characteristic diffraction peak was observed in the sample carbonized at 500 °C, indicating an amorphous state. When the carbonization temperature was increased to 800 °C, the peaks corresponding to the (002) and (100) diffractions of the graphitic framework appeared at approximately 22° and 44°, respectively. Therefore, carbon microparticles, with graphite crystals in the framework, were obtained at 800 °C using phenolic resin as a carbon precursor.

Figure 6 shows nitrogen adsorption isotherms of the carbon microparticles. The adsorption behavior of the sample carbonized at 1000 °C exhibited a type-II isotherm with a type-H4 hysteresis. Carbon materials with mixed micro- and meso-porosity usually show Type II isotherms [7, 21, 26]. The type-H4 hysteresis is often associated with narrow slit-like micropores [7, 26]. As stated above, graphitic carbon crystals were formed in the microparticle framework when the carbonization temperature was increased to 800 °C. As a result, lamellar planes of graphite carbon may have formed slit-like micropores. Brunauer–Emmett–Teller (BET) surface areas of carbon
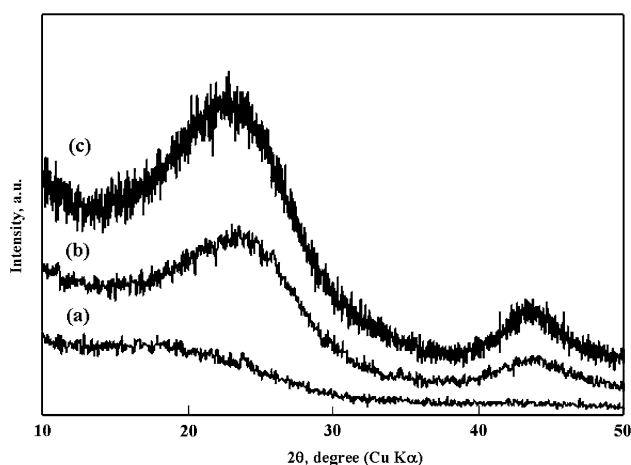
Fig. 5 XRD analysis for the samples carbonized at different temperatures: (**a**) 500 °C; (**b**) 800 °C; (**c**) 1000 °C
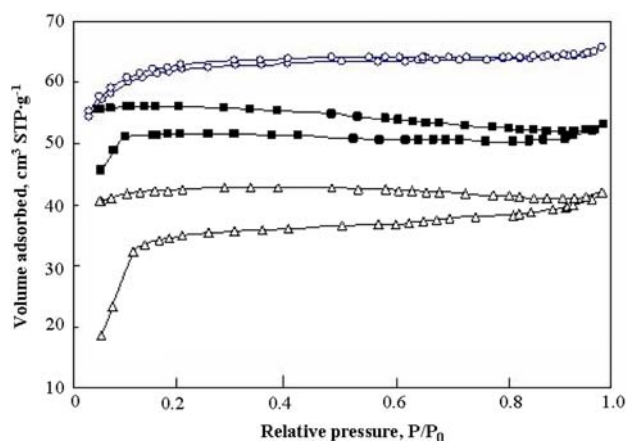

Fig. 6 Nitrogen adsorption isotherm of the samples carbonized at different temperatures: 500 °C (△); (b) 800°C (■); 1000 °C (○)

microparticles obtained by carbonization at 500, 800, and 1000 °C were 121, 202 and 213 m^2 g^{-1}, respectively.

### Carbonization and particle formation mechanism

Figure 7 shows the elemental carbon and hydrogen compositions and weight loss of the carbonaceous samples. The phenolic resins were 77.08 C wt% and 5.65 H wt% after drying at 160 °C for 1 h. With an increase in carbonization temperature, the carbon content of the samples increased from 88.92 wt% at 500 °C to 95.85 wt% at 1000 °C, while the hydrogen content decreased from 3.87 to 0.47 wt%. Most of the weight loss occurred below 500 °C and a less significant weight loss was observed between 800 and 1000 °C.

The phenolic resin solution completely infiltrated the air space of the SiO$_2$ inverse opal under reduced pressure due
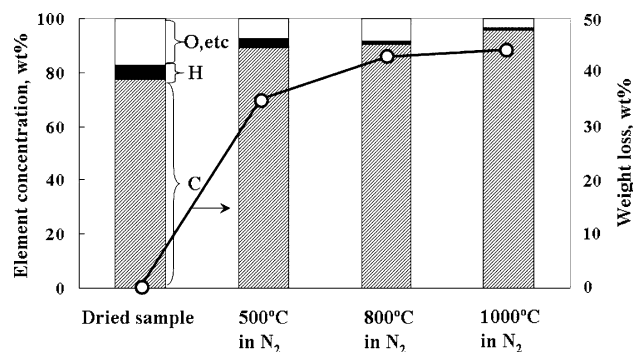

Fig. 7 Elemental composition of the samples and weight loss during the carbonization process (○).

to the high affinity between the surface of the SiO$_2$ inverse opal and the phenolic resin. When the phenolic-resin-infiltrated SiO$_2$ inverse opal was dried in air at 160 °C, the phenolic resin solidified on the surface of the SiO$_2$ inverse opal. In the carbonization process, polymerization, dehydrogenation, condensation, hydrogen transfer, and isomerization may have occurred at the surface of the SiO$_2$, according to the carbonization mechanism for phenolic resins indicated in Scheme 1 [27]. As a result, volumetric shrinkage of microparticles may have occurred radially from the center to the shell. As illustrated in Fig. 8, when the concentration of phenolic resin solution was low the particle, as well as the neck between the particles, became empty space. As a result, the synthesized carbon microparticles were hollow and had interlocked open windows. To the contrary, when the concentration of the phenolic resin solution was high, the phenolic resin completely filled the neck, at first due to the capillary force that resulted from drying, and then, during carbonization, the neck was filled by the carbon network. As a result, the shell of the particles was thick and strong. Although the microparticles appear to be filled, as shown in the Fig. 1, the center of the particles may have been hollow, as illustrated in Fig. 8b.
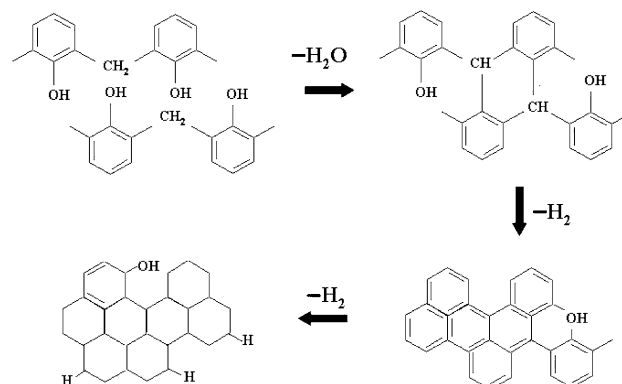
Scheme 1 Schematic representation of the carbonization mechanism for phenolic resins
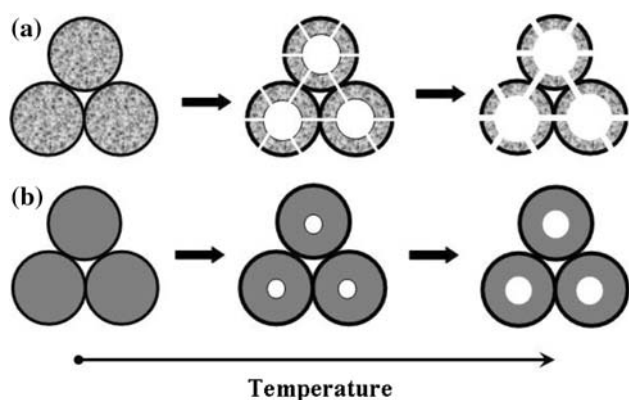
Fig. 8 Schematic representation for the section images due to shrinkage during carbonization. (**a**) phenolic resin solutions with low concentration were used; (**b**) phenolic resin solutions with high concentration were used

Conclusions

Well-defined carbon microparticle arrays with different particle morphologies were prepared in a one-step infiltration process under vacuum using phenolic resin as the carbon precursor and SiO_2 inverse opal as the template. Particle morphology varied with phenolic resin concentration and carbonization temperature. The morphology of carbon microparticles changed from particles with open windows to particles with filled interlocked bridges as the concentration of phenolic resin solution was increased. The carbon microparticles carbonized at 500 °C were in the amorphous state and the assembly had filled the interlocked bridges. The carbon microparticle assembly containing graphitic crystals formed at a carbonization temperature above 800 °C.

References

1. Lee J, Kim J, Hyeon T (2006) Adv Mater 18:2073
2. Wang Y, Liu Z, Han B, Huang Y, Yang G (2005) Langmuir 21:10846
3. Ma X, Xu F, Du Y, Chen L, Zhang Z (2006) Carbon 44:158
4. Gherghel L, Kubel C, Lieser G, Rader H, Mullen K (2002) J Am Chem Soc 124:13130
5. Lei Z, Xiao Y, Dang L, You W, Hu G, Zhang J (2007) Chem Mater 19:477
6. Wang Y, Su F, Lee JY, Zhao XS (2006) Chem Mater 18:1347
7. Lee KT, Lytle JC, Ergang NS, Oh SM, Stein A (2005) Adv Funct Mater 15:547
8. Fuertes AB (2003) J Mater Chem 13:3085
9. Tosheva L, Parmentier J, Saadallah S, Vix-Guterl C, Valtchev V, Patarin J (2004) J Am Chem Soc 126:13624
10. Su F, Zhao XS, Wang Y, Wang L, Lee JY (2006) J Mater Chem 16:4413
11. Xia Y, Gates B, Yin Y, Lu Y (2000) Adv Mater 12:693
12. Lopez C (2003) Adv Mater 15:1679
13. Braun PV, Rinne SA, Santamaria G (2006) Adv Mater 18:2665
14. Jiang P, Bertone JF, Colvin VL (2001) Science 291:453
15. Yang SM, Coombs N, Ozin GA (2000) Adv Mater 12:1940
16. Lei Z, Li J, Ke Y, Zhang Y, Zhang H, Li F, Xing J (2001) J Mater Chem 11:2930
17. Yi GR, Moon JH, Manoharan VN, Pine DJ, Yang SM (2002) J Am Chem Soc 124:13354
18. Wang H, Yu JS, Li XD, Kim DP (2004) Chem Commun 2352
19. Guan G, Kusakabe K, Ozono H, Taneda M, Uehara M, Maeda H (2007) Chem Eng J (in press), doi:10.1016/j.cej.2007.04.028
20. Zhou Z, Yan Q, Su F, Zhao XS (2005) J Mater Chem 15:2569
21. Su F, Zhao XS, Wang Y, Zeng J, Zhou Z, Lee JY (2005) J Phys Chem B 109:20200
22. Centeno TA, Vilas JL, Fuertes AB (2004) J Membr Sci 228:45
23. Cai Q, Huang ZH, Kang F, Yang JB (2004) Carbon 42:775
24. Waterhouse G, Waterlang MR (2007) Polyhedron 26:356
25. Bolhuis PG, Frenkel D, Mau SC, Huse DA (1997) Nature 388:235
26. Sing KSW, Everett DH, Haul RAW, Moscou L, Pierotti RA, Rouquerol J, Siemieniewska T (1985) Pure & Appl Chem 57:603
27. Funabiki K, Nakamura M, Tsuriya M (1981) Thermosetting Resins 2:220 (in Japanese)